Experimental Determination of the Melting Point and Heat Capacity for a Free Cluster of 139 Sodium Atoms

Martin Schmidt, Robert Kusche, Werner Kronmüller, Bernd von Issendorff, and Hellmut Haberland
Fakultät für Physik, Universität Freiburg, H. Herderstr. 3, D-79104 Freiburg, Germany
(Received 13 March 1997)

The heat capacity of a free cluster has been determined from the temperature dependence of its photofragmentation mass spectrum. The data for the spherical sodium cluster Na_N^+, with $N = 139$, show a maximum at 267 K, which is interpreted as the solid-to-liquid phase transition in this finite system. The melting point lies 104 K, or 28% lower than that of bulk sodium. The latent heat of fusion is reduced by 46%. [S0031-9007(97)03493-5]

PACS numbers: 64.70.Dv, 36.40.Ei, 36.40.Qv

The solid-to-liquid phase transition of finite sized systems differs in three main respects from that of its macroscopic limit: (1) The melting point decreases with decreasing particle size, (2) the phase transition is spread over a finite temperature range, and (3) the latent heat of fusion is reduced [1–15].

The problem of what remains of the bulk phase transition for finite systems has attracted a lot of experimental [1–5] and theoretical [6–17] interest. The reduction in melting temperature had been already observed by Pawlow [4] in 1909. It has been experimentally verified several times for supported clusters [1–3] and has been seen in many computer simulations [8–17]. The physical reason for the decrease in the melting point can be qualitatively understood in terms of the Lindemann criterion [18], which states that bulk matter will melt if the thermal fluctuations of the internuclear distance become larger than 10% to 15%. Assuming that a similar relation holds for clusters, one can argue that the many atoms on the cluster's surface are less constrained in their thermal movement, allowing larger fluctuations, which leads to a lower melting point. More formally correct arguments can be found in Refs. [6–17].

The reduction of the latent heat of fusion can be seen in numerical simulations [8,9] and has only very recently been experimentally observed for small Sn particles supported on an inert substrate [3]. The free sodium clusters studied here have a diameter of ~22 Å. They are about a factor of 5 smaller and contain over a factor of 100 fewer atoms than the smallest particle studied in Ref. [3]. Furthermore, a free particle in vacuum instead of one in contact with a surface is studied here.

A direct way to diagnose a phase transition is to look for some special feature of the heat capacity $c(T)$, which is defined as the partial derivative of the internal energy $U = U(T)$ with respect to the temperature T:

$$c(T) = \partial U/\partial T . \quad (1)$$

In the temperature range considered here, the bulk internal energy $U(T)$ is a nearly linear function of the temperature [see Fig. 1(a)], save for an abrupt jump at the melting temperature $T_{\mathrm{melt}} = 371$ K. Its magnitude is the latent heat of fusion, which is the energy needed to destroy the crystalline lattice at T_{melt}. The bulk heat capacity $c(T)$ [see Fig. 1(b)] is thus only weakly temperature dependent in this temperature range, save for a delta function at T_{melt}. The smoothing of the phase transition in finite sized particles has been calculated as in Ref. [14], and the results are included in Figs. 1(a) and 1(b), while in Fig. 1(c) the heat capacity of bulk sodium is compared to that of Na_{139}^+, which has been determined as described below. The peak of the experimental curve is interpreted

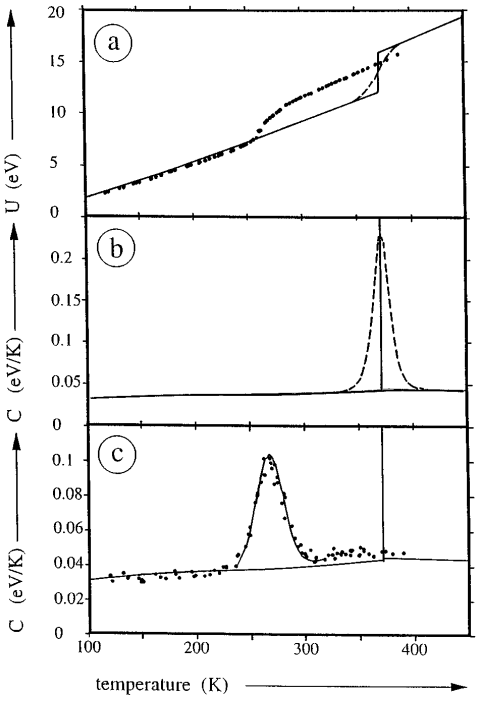

FIG. 1. Total internal energy $U(T)$ (a) of a 139 atom cluster and its heat capacity $c(T)$ (b) as a function of cluster temperature T, assuming the specific entropy of bulk sodium. The solid line is calculated neglecting the finite size of the particle. The dashed lines show the canonical result for a small particle, displaying the smoothing of the phase transition. The experimental data are shown by the solid points. Note the different vertical scales in (b) and (c).

as the melting point, which occurs at a lower temperature than the bulk one, as expected.

We do not know of any earlier experiment where the heat capacity near the solid-liquid phase transition was determined for a free cluster. Calculations of the heat capacity exist for smaller sodium clusters than those studied here [10,11]. Also, the heat capacities and caloric curves have been simulated for Cu and Au clusters [12,13]. Experimentally, melting of large sodium clusters (10^3 to 10^4 atoms per cluster) has been studied earlier [19]. Melting has also been deduced earlier from changes in the spectral characteristics of free clusters composed of a large molecule embedded in rare gas atoms [7,8]. For small sodium clusters ($n \leq 15$) the temperature dependence of the optical spectrum was measured as reported earlier [20]. No spectral feature due to a phase transition could be identified, although a thorough search was made by measuring the optical spectra every 20 K [21,22]. The heat capacity of free Fe, Co, and Ni clusters was determined in a study of the ferromagnetic phase transition [23].

The basic process used to measure the heat capacity is the temperature dependence of the photofragmentation pattern of a size selected cluster ion:

$$\mathrm{Na}_N^+(T) \; + \; n\,\hbar\omega \longrightarrow \mathrm{Na}_{N-x}^+ \; + \; x\mathrm{Na}\,, \qquad (2)$$

where n photons are absorbed sequentially, and x neutral sodium atoms are emitted [24]. The number $x = x(T, n)$ can be easily determined from the experiment described below. The total energy of Eq. (2) can be written as

$$U^*(T, n) \; = \; U(T) \; + \; n\,\hbar\omega\,. \qquad (3)$$

There are two ways to increase $U^*(T, n)$ and thus the number of ejected atoms: (1) One can directly add an amount of *energy* δU by changing the number or the energy of the photons absorbed. (2) One can heat the cluster before laser irradiation, thus changing its *temperature* by δT. If δU and δT are chosen such that the number of additionally ejected atoms is the same, one has $U(T + \delta T) = U(T) + \delta U$. The heat capacity can then be calculated by replacing the differentials in Eq. (1) by the finite differences δU and δT.

In other words, the cluster itself is used as an ultrasensitive calorimeter. Energy is supplied either thermally or by photons ($E = \hbar\omega \approx 10^{-18}$ J). That the same internal energy is reached is monitored by the number of ejected atoms.

Two experimental tools are needed in order to measure the heat capacity in this way: First, a beam of cluster ions of known and variable temperature has to be produced, as shown in Fig. 2. The clusters are thermalized by 10^5 to 10^6 collisions with the He buffer gas. They acquire a canonical distribution of internal energy, which they retain once they leave the thermalization chamber through a 6 mm hole [20,25]. Second, a tandem time-of-flight mass spectrometer (see Fig. 3) is used to measure the photofragment mass spectra in steps of 1 K between 100 and 450 K at a fixed photon energy. Care was taken as to change $U(T)$ as little as possible on the way between source and laser interaction [21].

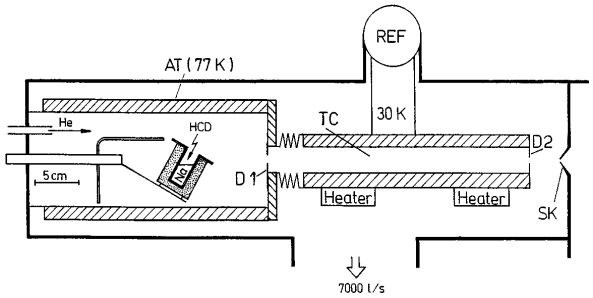

FIG. 2. Temperature controlled cluster ion source. Helium gas is flowing into a liquid nitrogen cooled aggregation tube (AT). Sodium is evaporated from a small container. Charged particles are produced by a hollow cathode gas discharge (HCD), using the Na container as cathode. Clusters, which probably grow preferentially around the charged particles, are transferred through a first diaphragm (D1) into the thermalization chamber (TC), the temperature of which can be varied between 35 and 600 K. REF = closed cycle refrigerator. The cluster pass through D2 and a skimmer (SK) into the next vacuum chamber containing TOF1, as shown in Fig. 3.

Four mass spectra are shown schematically in Fig. 4. The top figure shows a spectrum without photon interaction. Only the cluster mass selected by TOF1 is visible [25]. The photon energy is chosen such that four neutral atoms are ejected per photon. At temperature T_1 the first three peaks to the left of the initially selected cluster result from the absorption of a certain number, say n, of photons. The width of the mass distribution stems from the thermal distribution of the selected cluster ion and the statistical nature of the fragmentation process. The next group of three masses results from the absorption of $n + 1$ photons, etc. Increasing the cluster temperature results in additional evaporated atoms. The distributions shift to smaller cluster sizes, as indicated by the arrows in Fig. 4. Temperature T_2 shows an intermediate case, while at T_3 the intensity maxima are at the same masses as for T_1. The effect of the additional temperature

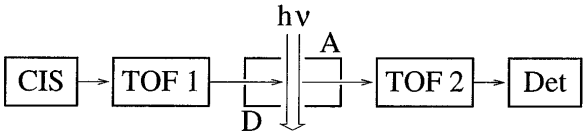

FIG. 3. Schematic of the machine. The cluster ion source (CIS) is shown in more detail in Fig. 2. It produces a large variety of different cluster sizes, so that a first time-of-flight (TOF1) mass spectrometer is necessary to select one size, say Na_{139}^+. Photons are absorbed from a laser beam and the photofragmentation mass spectrum is recorded by TOF2. A deceleration/acceleration (D/A) stage is added, so that TOF2 can record the complete fragmentation spectrum. Both TOFs are of the reflectron type having mass resolutions of 1500 and 800, respectively. Det = Detector.

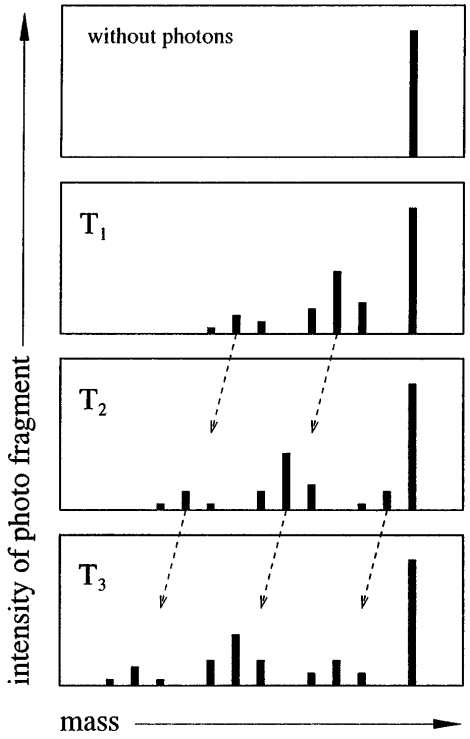

FIG. 4. Schematic photofragmentation mass spectra as a function of the heat bath temperature. See text for details.

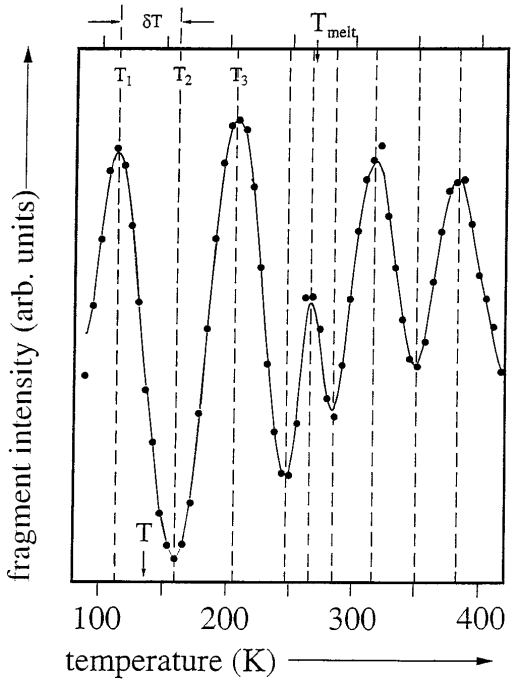

FIG. 5. Intensity of the fragment Na^+_{136} as a function of the temperature of the initially selected Na^+_{139}. The position of the extrema is indicated by the vertical dashed lines. δT decreases in the vicinity of the melting point. The smaller δT gives, via Eq. (4), a larger c.

$\delta T = T_3 - T_1$ is consequently the same as that of an additional photon energy $\delta U = \hbar\omega$.

Figure 5 shows the experimental intensity of one photofragment (Na^+_N, with $N = 136$, i.e., $x = 3$ sodium atoms lost) as a function of the initial cluster temperature. A maximum in this plot means that one of the maxima seen in Fig. 4 has reached this photofragment. A minimum, on the other hand, implies that the selected mass is exactly in between two such distributions. The energetic difference between maximum and minimum is consequently $\hbar\omega/2$. The mean heat capacity in the temperature range between maximum and minimum can now be deduced by dividing the energetic by the thermal difference:

$$c(T) \approx \frac{\delta U}{\delta T} = \frac{\hbar\omega/2}{T_2 - T_1}, \qquad (4)$$

with $T = (T_1 + T_2)/2$. This procedure is repeated for all maxima and minima of the many observed cluster fragments. Note that there are no adjustable parameters in this procedure.

The cluster Na^+_{139} was chosen for this exploratory study. It has 138 valence electrons and is thus spherically symmetric in the jellium approximation, which should be rather good for this cluster size [26]. The experimental result for the heat capacity is shown in Fig. 1(c).

There is one assumption inherent in this procedure, namely that the photon-induced excitation relaxes completely into a statistical equilibrium before an atom is ejected. Otherwise, the number of ejected atoms would not only depend on U^*, i.e., the sum of the two terms in Eq. (3), but explicitly on their relative magnitudes. The validity of the assumption was checked by using two different photon energies $\hbar\omega = 2.7$ and 3.1 eV. This gives different δT values in Fig. 5 and Eq. (4) but the same experimental result, within experimental error [21].

The width of the $c(T)$ curve is only slightly broadened by using the finite differences of Eq. (4), instead of the differentials in Eq. (1). The values for δT can be read off Fig. 5, and assuming that $c(T)$ is given by a Gaussian in the neighborhood of the melting point, $c = q \exp[-(T - T_{\mathrm{melt}})^2/2\Delta^2]/(\Delta\sqrt{2\pi})$, one can unfold the data. This gives the solid curve in Fig. 1(c), which very nearly goes through the data points. From a fit one obtains $q = 1.98$ eV and $T_{\mathrm{melt}} = 267$ K. The experimentally determined width of the phase transition ($\Delta = 12.6$ K) is 4.7 K larger than that calculated from the bulk value prediction given in Fig. 1(b). This additional broadening is probably caused by the reduction of the latent heat, since the width of phase transitions in finite systems depends on the latent heat [9,21].

The experimentally determined melting point is shifted by 104 K, or 28%, to lower temperatures compared with the bulk melting point. The integral of the experimental curve ($q = 1.98$ eV) is equal to the latent heat. It is smaller than the bulk value (3.69 eV), since the cohesive energy has not yet reached its bulk value for these cluster

sizes [24]. The caloric curve $U(T)$ was calculated by integration of $c(T)$. The integration constant was chosen by extrapolating the heat capacity down to 0 K, in analogy to the bulk curve. The result is included in Fig. 1(a). Measurements on other sizes of sodium clusters are in progress, and will be published elsewhere [21]. The combined statistical and reproducibility error for T_{melt} is ± 2 K, while it is ± 1.5 K and ± 0.15 eV for Δ and q, respectively.

In summary, a calorimetric method has been described which allows the measurement of the heat capacity of a free, mass selected cluster. A beam of cluster ions is generated, which has a canonical distribution of internal energy. One cluster size is selected, irradiated by photons of known energy, and the photofragmentation mass spectrum is measured as a function of cluster temperature. Using Eq. (4) one can determine the temperature dependence of the heat capacity. This was done for the spherically symmetric sodium cluster Na_{139}^{+}, and a reduction of the melting point by 28%, compared to the bulk value, is observed. The latent heat of fusion is reduced by 46%, while the width of the solid-to-liquid transition is increased by 59% with respect to a bulk like system consisting of 139 atoms.

This work has been supported by the Deutsche Forschungsgemeinschaft through SFB 276.

[1] D. A. Buffat and J. P. Borel, Phys. Rev. A **13**, 229 (1976).
[2] Y. Leereah, G. Deutscher, P. Cheyssac, and R. Kofman, Europhys. Lett. **12**, 709 (1990).
[3] S. L. Lai, J. Y. Guo, V. Petrova, G. Ramanath, and L. H. Allen, Phys. Rev. Lett. **77**, 99 (1996).
[4] P. Pawlow, Z. Phys. Chem. **66**, 545 (1909).
[5] M. Takagi, J. Phys. Soc. Jpn. **9**, 361 (1954).
[6] M. E. Fischer, in *Critical Phenomena*, Proceedings of the International School of Physics "Enrico Fermi," Course LI (Academic Press, New York, 1971), p. 73.
[7] J. Jortner *et al.*, in *The Chemical Physics of Atomic and Molecular Clusters*, Proceedings of the International School of Physics "Enrico Fermi," Course CVII (Academic Press, New York, 1990), p. 43.
[8] S. Berry, in *Clusters of Atoms and Molecules I*, edited by H. Haberland, Springer Series in Chemical Physics Vol. 52 (Springer-Verlag, Berlin, 1994), Chap. 2.8. See also Ref. [7], p. 23.
[9] P. Labastie and R. L. Whetten, Phys. Rev. Lett. **65**, 1567 (1990).
[10] R. Poteau, F. Spiegelmann, and P. Labastie, Z. Phys. D **30**, 57 (1994).
[11] N. Ju and A. Bulgac, Phys. Rev. B **48**, 2721 (1993).
[12] X. Yu and P. M. Duxbury, Phys. Rev. B **52**, 2102 (1995).
[13] O. H. Nielsen, J. P. Sethna, P. Stoltze, K. W. Jacobsen, and J. K. Norskov, Europhys. Lett. **26**, 51 (1994).
[14] H. Cheng, X. Li, R. L. Whetten, and R. S. Berry, Phys. Rev. A **46**, 791 (1992).
[15] R. M. Lynden-Bell, Mol. Phys. **86**, 1353 (1995).
[16] P. A. Hervieux and D. H. E. Gross, Z. Phys. D **33**, 295 (1995).
[17] J.-B. Maillet, A. Boutin, and A. H. Fuchs, Phys. Rev. Lett. **76**, 4336 (1996).
[18] The Lindemann criterion is well fulfilled for bulk material. It has not been proven theoretically, but shown to be physically reasonable in molecular dynamics simulations, e.g., W. A. Curtis and N. W. Ashcroft, Phys. Rev. Lett. **56**, 2775 (1986); Ref. [8].
[19] T. P. Martin, Phys. Rep. **273**, 201 (1996).
[20] Ch. Ellert, M. Schmidt, Ch. Schmitt, Th. Reiners, and H. Haberland, Phys. Rev. Lett. **75**, 1731 (1995).
[21] M. Schmidt, R. Kusche, and H. Haberland (to be published).
[22] Martin Schmidt, Ph.D. thesis, Freiburg, 1996 (unpublished).
[23] D. Gerion, A. Hirt, I. M. L. Billas, A. Châtelain, and W. A. de Heer, in *Proceedings of the 8th International Symposium on Small Particles and Inorganic Clusters (ISSPIC8), Copenhagen, 1996*, book of abstracts, edited by P. E. Lindelof (University of Copenhagen, Denmark); I. Billas (private communication).
[24] C. Bréchignac, Ph. Cahuzac, F. Carlier, M. de Frutos, and J. Leygnier, Z. Phys. D **19**, 1 (1991); C. Bréchignac, in Ref. [8], Chap. 4.1.
[25] At high enough temperatures one sees "metastable" fragments in the mass spectra due to atom emission in the drift zone of TOF1, which can easily be taken care of in the data analysis [21].
[26] M. Brack, Rev. Mod. Phys. **65**, 677 (1993); W. A. de Heer, Rev. Mod. Phys. **65**, 611 (1993).